FERROMAGNETIC CORE-SHELL COAXIAL NANOSTRUCTURES ON GALLIUM ARSENIDE SUBSTRATES

E. V. MONAICO[1,*], V. MORARI[2], M. KUTUZAU[3,4], V. V. URSAKI[1,5], K. NIELSCH[3], I. M. TIGINYANU[1,5]

[1] National Center for Materials Study and Testing, Technical University of Moldova, 2004 Chisinau, Moldova
E-mails: eduard.monaico@cnstm.utm.md; vvursaki@gmail.com
[2] Institute of Electronic Engineering and Nanotechnologies "D. Ghitu", 2028 Chisinau, Moldova
[3] Institute for Metallic Materials (IMW), Leibniz Institute of Solid State and Materials Research (IFW Dresden), Helmholtzstr 20, 01069 Dresden, Germany
[4] Electrochemical Sensors and Energy Storage, Institute of Chemistry, Faculty of Natural Sciences, Chemnitz University of Technology, Straße der Nationen 62, 09111 Chemnitz, Germany
[5] Academy of Sciences of Moldova, 2001 Chisinau, Moldova

Received May 18, 2022

Abstract. Fe and NiFe coatings have been electrochemically deposited on GaAs nanowires arrays prepared by electrochemical etching of (001) and (111)B GaAs substrates in a 1M HNO_3 electrolyte. It was found that deposition in galvanostatic mode is preferable for Fe coatings, while it is not suitable for NiFe alloys. Potentiostatic deposition was applied for $Ni_{0.65}Fe_{0.35}$ coatings. The fabricated ferromagnetic coaxial core-shell structures have been investigated by means of *scanning electron microscopy* (SEM) and *vibrating sample magnetometry* (VSM). A comparative analysis of magnetic properties of the produced structures in terms of saturation and remanence moment, squareness ratio, and coercivity, was performed between planar and coaxial structures, between Fe and NiFe coatings, as well as between different orientations of the magnetic field with respect to the nanowires axis.

Key words: Nanowires; nanotubes; core-shell structures; anodization; electroplating; hysteresis loop; magnetic anisotropy; magnetic properties of interfaces.

1. INTRODUCTION

Various arrays of ferromagnetic nanostructures including wires, core-shell structures and tubes, present interest for a wide range of applications, such as high-density data storage, microelectronics, spintronics and microwave devices [1, 2]. Properties of these quasi-one-dimension structures are strongly dependent on their dimensions, shape anisotropy, and selected material. Tubular arrays and coaxial core-shell structures offer advantages over *nanowires* (NWs), owing to possibilities to vary the thickness of the tube wall or the shell in addition to the control of the length and diameter [3–6].

Nanoscale magnetic structures are usually produced with high precision by direct writing assisted by a *focused electron beam* (FEB), or lithographic techniques

using *ion beams* (IBL) and two-photon technologies [6–8]. However, these technologies are expensive and their throughput is low. Much more simple, efficient, and low-cost are template assisted electrodeposition methods, which also are widely used for the fabrication of different architectures based on nanowire and nanotube arrays.

Nano-templates with well-defined pore architecture, including templates with ordered arrangement of pores, are used for production of structures with excellent control over geometrical features and morphology. Magnetic arrays with desired aspect ratio, composition, structure, morphologies and density are produced by these methods, which ensure tunable magnetic, magneto-transport and thermoelectric properties [4].

Ion track-etched polymers and porous anodic membranes are among the most commonly used templates for the fabrication of magnetic arrays by means of electrochemical deposition inside the pores [1, 4]. Among such membranes, aluminum oxide (AAO) templates are of especial interest, due to their versatile fabrication technique allowing easy tuning of pore diameter, length, and inter-pore distances [1]. Nanomagnetic arrays, including nanowires, nanocylinders, and core-shell structures with controlled parameters, have been prepared by deposition in AAO templates. However, the produced arrays are always oriented perpendicularly to the substrate surface, *i.e.* they are out of the substrate plane. As a result, they are anisotropic with respect to the plane perpendicular to the template surface, but they are isotropic for the in-plane magnetization.

Technological methods have been recently developed for preparation of templates with pores oriented both perpendicular and parallel to the top substrate surface [9, 10], as well as technological routes for filling these templates with metallic nanotubes or nanodots [10–12].

The goal of this paper is to deposit ferromagnetic Fe and NiFe shells on GaAs nanowire arrays oriented both in-plane and out-of-plane with the substrate, by making use of electrochemical etching technologies previously developed for this purposes [13, 14], and to compare their magnetic properties in terms of composition, magnetic metal deposition mode, and orientations of the magnetic field with respect to the nanowires axis.

2. MATERIALS AND METHODS

(111)-oriented and (001)-oriented *n*-type GaAs wafers with free electron concentrations of 2×10^{18} cm^{-3} and 1×10^{18} cm^{-3}, respectively, were used in experiments. The wafers were cleaved into 1×1 cm^{-2} chips, which were sonicated in acetone for 10 min, rinsed in distilled water and dried. They were also subjected to wet chemical etching in HCl/H_2O with a ratio of (1:3) for 2 min in order to remove the native oxide from the surface before the anodization. The anodization was carried out on the (001) and (111)B surfaces of GaAs in 1M HNO_3 electrolyte

at applied anodic potential of 4 V in an electrochemical cell with three electrodes configuration. Each of the chips prepared according to the above described procedure served as *working electrode* (WE). A mesh from Pt wire with the total surface of 6 cm^2 was used as *counter electrode* (CE), while a saturated Ag/AgCl served as *reference electrode* (RE). Etching was performed for 15 min, resulting in an array of nanowires with the length of 45 μm oriented predominantly perpendicularly to the substrate surface for (111)B GaAs samples, whereas nanowires with a length up to 180 μm oriented predominantly parallel to the substrate surface were formed in (001) GaAs samples.

Deposition of Fe on the GaAs nanowires array as well as on non-etched GaAs wafers serving as WE was carried out in the galvanostatic mode at current density of 2 mA/cm^2 in a cell with three-electrode configurations [15]. Saturated Ag/AgCl and Pt wires were used as RE and CE, respectively. The samples were kept in NH_3 for 10 s and in H_2O for 10 s before metal deposition. The electrolyte consisted of 0.01 mol/L iron sulfate ($FeSO_4$), 0.03 mol/L ammonium sulfate ($(NH_4)_2SO_4$), and 0.3 mol/L sodium sulfate (Na_2SO_4), with pH of 5.1. The deposition was performed under the control of a computer *via* a Biologic VSP-128 device for a period of time between 10 and 20 s.

Deposition of $Ni_{0.65}Fe_{0.35}$ coatings was carried out in an electrochemical cell with three electrodes in the potentiostatic mode at applied potential of – 4 V *vs saturated calomel electrode* (SCE) for a period of time between 20 and 60 s in electrolyte solution containing $NiSO_4 \cdot 6H_2O$ (103 g/L), $NiCl_2 \cdot 6H_2O$ (5 g/L), $FeSO_4 \cdot 7H_2O$ (4.8 g/L), H_3BO_3 (25 g/L), and $C_6H_8O_6$ (3 g/L) with pH value of 3 [16]. A Pt cage was used as counter electrode and SCE as reference electrode, while sample served as working electrode connected and fully controlled *via* a Biological SP-50 device. One should mention that the deposition in the galvanostatic mode is not suitable for NiFe alloys on porous materials (GaAs nanowires in our case), because of non-uniform deposition and formation of separate Ni and Fe nanoparticles. The porous materials are characterized by a high specific surface, leading to a high susceptibility of the metal ions deposition to changes in the flowing currents. In order to avoid miscalculations of the needed applied current density on porous surface, the electrodeposition of NiFe was carried out in the potentiostatic mode for both planar substrates and GaAs nanowire arrays. On the other hand, the potentiostatic deposition is a more slow process as compared with the galvanostatic deposition mode, three time longer processes being necessary to reach the same coating thickness.

The morphology of the prepared samples was studied using a LEO-ZEISS Gemini 1530 *scanning electron microscope* (SEM).

The magnetization curves of coaxial core-shell magnetic nanostructures were investigated by a *vibrating sample magnetometer* (VSM) from Quantum Design VersaLab™ with applied magnetic fields of up to ±3 T at room temperature. Investigations have been carried out in both in-plane (ip) and *out-of-plane* (oop) configurations.

3. RESULTS AND DISCUSSION

With the purpose of comparison, the magnetic properties of coaxial core-shell structures were compared with those of magnetic metal properties on planar GaAs wafers. As mentioned above, deposition should be carried out for a longer time with potentiostatic mode, as compared to the galvanostatic mode, in order to reach similar coating thickness. The morphology of NiFe coating on a (111)B GaAs wafer after 60 s of potentiostatic deposition represents a quite uniform nanoporous layer with randomly distributed grains with dimensions up to 200 nm, also having a nanoporous structure (Fig. 1a).

Anodization of (111)B substrates in 1M HNO_3 electrolyte for 15 min results in the formation of an array of nanowires oriented preponderantly perpendicularly to the substrate surface as shown in previous publications [13]. The produced nanowires have a stoichiometric GaAs composition with a high crystalline quality, as indicated by narrow XRD reflexes. The nanowires preserve the initial (111)B crystallographic orientation of the sample, as indicated by the predominance of (111) and (333) reflexes in the XRD pattern [13]. The morphology of potentiostatically deposited coating on such a GaAs wire array have nanoporous morphology similar to that observed on planar (111)B substrates (Fig. 1b).

Deposition of Fe in galvanostatic mode results in the formation of denser nanoparticles with sizes up to 100 nm as illustrated for a coating on (001) GaAs substrate after 20 s deposition (Fig. 1c).

Anodization of (001) GaAs substrates in 1M HNO_3 electrolyte results in the formation of an array of nanowires oriented preponderantly parallel to the substrate surface as shown in a recent paper [14]. The Fe galvanostatic deposition on such nanowires also results in the formation of nanoparticles, which sizes and density increase with increasing the deposition time. For instance, separated nanoparticles are deposited after 10 s electroplating as illustrated in Fig. 1d, while the GaAs nanowires are totally covered by Fe nanoparticles after 20 s deposition as shown in Fig. 1f.

Figures 1e and 1f compare the Fe coating obtained after 15 s deposition on a GaAs nanowire produced on (111)B GaAs substrate with that obtained after 20 s deposition on a GaAs nanowire produced on (001) GaAs, respectively.

Figure 2 presents hysteresis loops measured in out-of-plane (curves 1–3) an in-plane (curves 4–6) configurations on NiFe coatings deposited in potentiostatic mode on (111)B GaAs substrates for different periods of time from 20 s to 60 s. One can see that the magnetic moment increases with increasing the deposition time for both in-plane and out-of-plane configurations, the moment being higher for the in-plane configuration. The same is true for the coercive forces, which also increase with increasing the deposition time, and they are higher for the in-plane configuration. However, the largest difference between the in-plane and out-of-plane configurations is noticed for the remanence ratio M_r/M_s = RR (squareness),

which is around 0.65 for the in-plane configuration, and is only around 0.1 for the out-of-plane configuration.

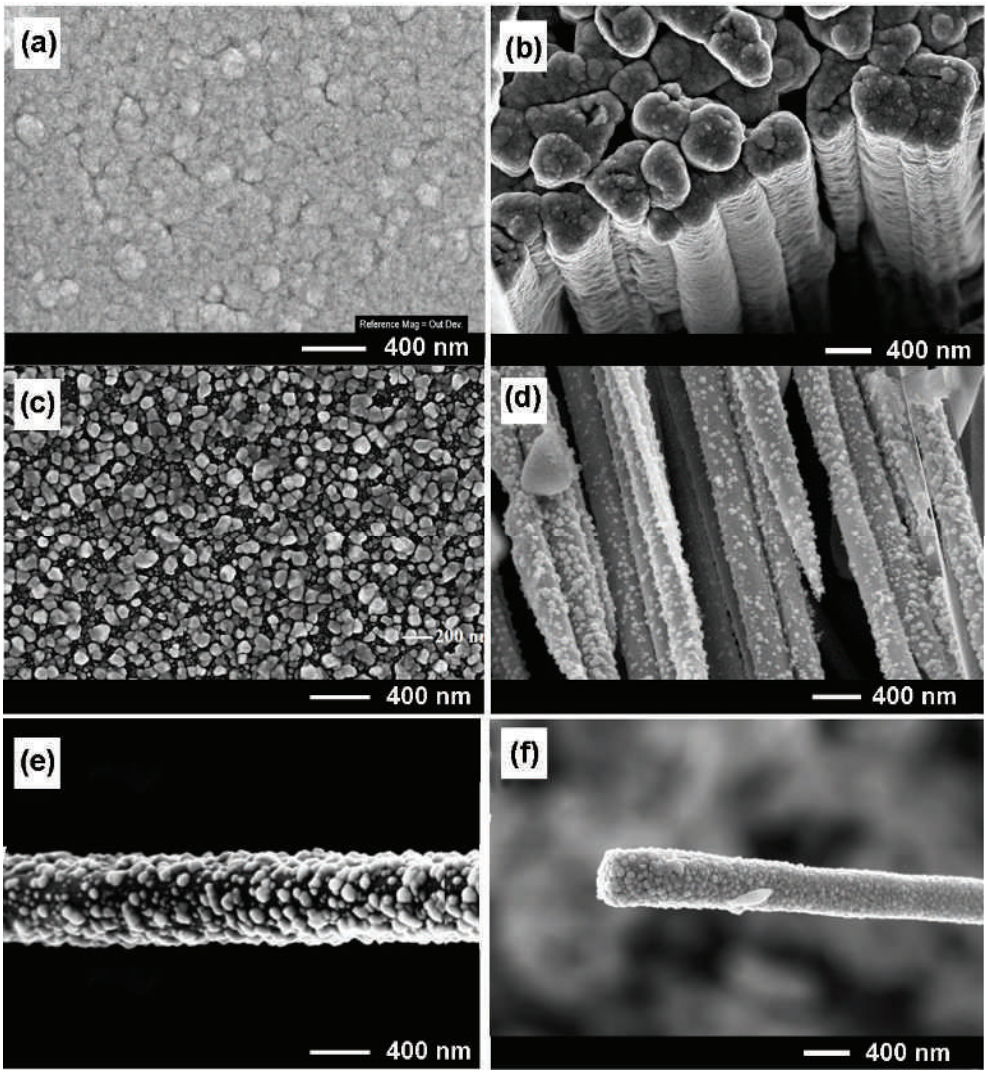

Fig. 1 – (a) SEM image of a NiFe coating on (111)B GaAs wafer deposited for 60 s. (b) SEM image of GaAs nanowire array prepared by anodization of (111)B GaAs wafer with applied voltage of U = – 4V coated with a NiFe layer for 60 s. (c) SEM image of a Fe coating on (001) GaAs wafer deposited for 20 s. (d) SEM image of GaAs nanowire array prepared by anodization of (001) GaAs wafer covered by a Fe coating deposited for 10 s. (e) SEM image of a GaAs nanowire prepared by anodization of (111)B GaAs wafer covered by a Fe coating deposited for 15 s. (f) SEM image of a GaAs nanowire prepared by anodization of (001) GaAs wafer covered by a Fe coating deposited for 20 s.

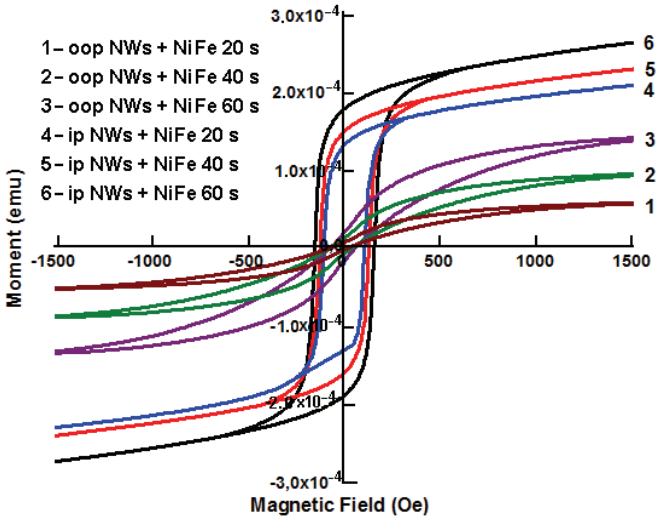

Fig. 2 – Hysteresis loops measured in in-plane (ip) and out-of-plane (oop) configurations on (111)B GaAs wafers.

Figure 3 shows the hysteresis loops measured in in-plane (a) an out-of-plane (b) configurations on nanowires array prepared on (111)B GaAs substrates with NiFe coatings deposited in potentiostatic mode for different periods of time from 20 s to 60 s. One can see that, similarly to the NiFe coatings on planar GaAs substrate, the magnetic moment increases with increasing the deposition time for both the in-plane and out-of-plane configurations. However, as compared with planar coatings, the increase of coercivity with increasing the deposition time is much more significant for nanowires with NiFe coatings. At the same time, there is not such a big difference in the remanence ratio for the in-plane and out-of-plane configurations.

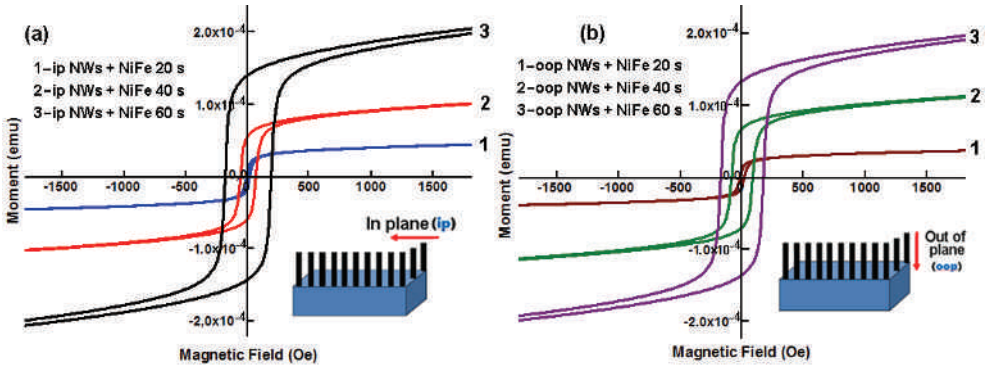

Fig. 3 – Hysteresis loops measured in in-plane (a) and out-of-plane (b) configurations on GaAs/NiFe core-shell arrays prepared on (111)B GaAs wafers.

With the purpose of comparison of magnetic properties of NiFe and Fe coatings on GaAs nanowires array, Fig. 4a shows hysteresis loops measured in in-plane an out-of-plane configurations on nanowires array prepared on (111)B GaAs substrates with Fe coatings deposited in galvanostatic mode for 20 s. If one compares the hysteresis loops in Fig. 3 and Fig. 4a, one can notice that the magnetic moment as well as the coercivity of GaAs nanowires coated with Fe for 20 s in the galvanostatic mode is higher than that of nanowires coated with NiFe for 60 s in the potentiostatic mode. Figure 4b presents the hysteresis loops for GaAs nanowires prepared on a (001) GaAs substrate coated with Fe.

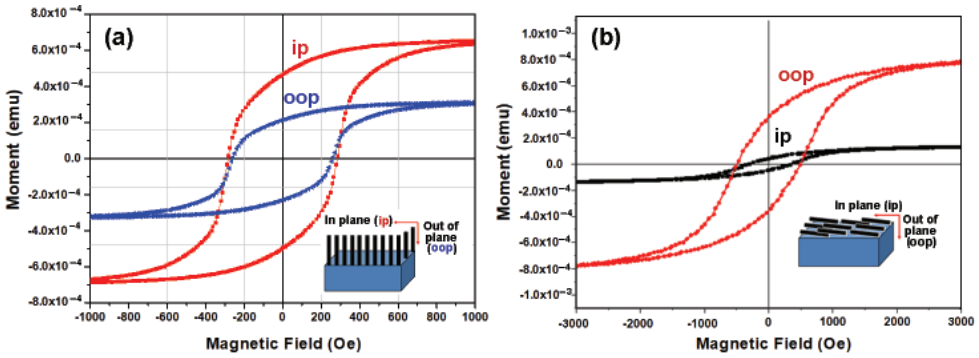

Fig. 4 – Hysteresis loops measured in in-plane and out-of-plane configurations on GaAs/Fe core-shell arrays prepared on (111)B GaAs wafers (a), and on (001) wafers (b), after galvanostatic deposition of Fe for 20 s.

Note that for nanowires prepared on (111)B GaAs substrates, which are oriented perpendicularly to the substrate, the magnetic field is applied perpendicularly to the nanowire array in the case of in-plane configuration, and along the nanowires axis in the case of out-of-plane configuration. For nanowires prepared on (001) GaAs substrates which are oriented parallel to the substrate surface, the orientation of the magnetic field with respect to the direction of nanowires is *vice-versa*, *i.e.* the magnetic field is oriented perpendicularly to the nanowire axis for the out-of-plane configuration.

The magnetic characteristics of the investigated samples are summarized in Table 1. The analysis of data in this table suggests that for planar coatings the magnetic properties, namely the coercive force and the remanence ratio, are better for the in-plane configuration than for the out-of-plane configuration, for both (111)B and (001) GaAs substrates, as well as for both NiFe coatings deposited in the potentiostatic mode and Fe coating deposited in the galvanostatic mode. For instance, the coercive force is 66 Oe for out-of-plane configuration and 153 Oe for in-plane configuration for NiFe coatings with 60 s time deposition. The remanence ratio is 0.13 for out-of-plane configuration and 0.67 for in-plane configuration, for this coating. A similar behavior is also noticed for planar Fe coatings on both (111)B and (001) GaAs substrates.

Table 1

Saturation moment, remanence and coercive forces for electrochemically deposited NiFe and Fe coatings on planar substrates and GaAs nanowires samples for in-plane and out-of plane VSM measurements

Crystallographic orientation	Sample description	Deposition mode	Saturation moment, M_s (emu) $\times 10^{-4}$		Remanence, M_r (emu) $\times 10^{-4}$		Coercive force, H_c (Oe)	
			ip	oop	ip	oop	ip	oop
(111)B GaAs	Planar/NiFe	Potentiost. 20s	2.01	0.55	1.28	0.05	107	45
	Planar/NiFe	Potentiost. 40s	2.27	0.92	1.46	0.10	126	57
	Planar/NiFe	Potentiost. 60s	2.61	1.37	1.75	0.18	153	66
(111)B GaAs	Nanowires/NiFe	Potentiost. 20s	0.45	0.37	0.08	0.11	9	16
	Nanowires/NiFe	Potentiost. 40s	1.02	1.11	0.57	0.69	60	84
	Nanowires/NiFe	Potentiost. 60s	2.03	1.94	1.41	1.34	184	172
(111)B GaAs	Planar/Fe	Galvanost. 20s	6.50	0.52	2.67	0.19	89	71
	Nanowires/Fe	Galvanost. 20s	6.60	3.1	4.65	2.1	284	260
(001) GaAs	Planar/Fe	Galvanost. 20s	5.10	1.60	2.00	0.20	305	170
	Nanowires/Fe	Galvanost. 20s	1.34	7.75	0.46	3.62	330	500

The magnetic parameters are better for NiFe and Fe coated nanowires as compared to planar structures. The coercivity is larger than 170 Oe for both magnetic field configurations on GaAs nanowires coated with NiFe for 60 s in the potentiostatic mode, while the remanence ratio is around 0.7 for both configurations. The same remanence ratio of around 0.7 is measured for both magnetic field configurations on GaAs nanowires prepared on (111)B GaAs substrates and coated with Fe for 20 s in the galvanostatic mode, while the coercivity is by a factor of around 3 larger than that measured on planar structures with the same coating. The largest value of coercivity (around 500 Oe) was reached on GaAs nanowires prepared on (001) GaAs substrates, when measured with out-of-plane magnetic field configuration, *i.e.* with the magnetic field perpendicular to the nanowires axis. However, the remanence ratio is around 0.5 for this case, which is less than 0.7 measured for NiFe and Fe coatings on nanowires prepared on (111)B GaAs substrates.

Generally, the coercive force is little larger with magnetic field perpendicular to the nanowire axis as compared with magnetic field parallel to the nanowire, for thick enough magnetic metal coatings. This observation is some-how different from the behavior previously noticed in small diameter thin ferromagnetic nanotubes. It was shown that in ferromagnetic Co nanowires with small diameters (26 nm) [17] and in Ni nanotubes with diameter of 35 nm [18], the coercive force is higher for the magnetic field applied in the direction of the wire axis, as compared with the perpendicular direction, *i.e.* the longitudinal coercivity $H_{c\parallel}$ is larger than the transverse coercivity $H_{c\perp}$. It was also found that in Ni and Co nanotubes the ratio of $H_{c\parallel}/H_{c\perp}$ decreased from 2.1 (for Ni) and 1.4 (for Co) to the value of around 1 for nanotubes of both materials, when the diameter of nanotubes increased from 35 nm to 160 nm

[19]. There are two essential differences between the core-shell coaxial structures prepared in this work on GaAs nanowires and previously investigated magnetic nanowires and nanotubes. One of them is related to differences in geometrical parameters, and another one refers to differences in crystalline structure. Previously investigated nanotubes were basically single crystalline, while the ferromagnetic shell in the prepared core-shell structures exhibit a granular morphology as illustrated by images in Fig. 1.

The magnetic anisotropy in crystalline ferromagnetic nanowires and nanotubes has been previously discussed in terms of movement of different types of domain boundaries: vortex wall and transverse wall [20, 21]. It was found that in thin tubes the vortex domain wall is preferred, while in thick tubes the transverse domain wall dominates. The situation seems to be more complicated in the case of polycrystalline tubular structures with nanograin morphology. The movement of different types of domain walls in such structures, apart from geometrical parameters, is influenced additionally by the nanograin boundaries.

4. CONCLUSIONS

Uniform nanogranular Fe and NiFe layers have been electroplated on both planar substrates and nanowire arrays prepared by anodization of GaAs substrates. Fe layers were easily deposited in the galvanostatic mode, while deposition in the potentiostatic mode was preferable for deposition of NiFe coatings. Three time longer deposition was necessary in the potentiostatic mode to reach the same coating thickness as with galvanostatic deposition. Planar structures exhibited anisotropy of the coercivity and the remanence ratio with respect to the orientation of the magnetic field, the magnetic parameters being higher for the in-plane configuration as compared to out-of-plane configuration. The magnetic parameters for both Fe and NiFe coatings were found to be higher for coaxial core-shell structures as compared to planar structures, while the magnetic anisotropy was less pronounced. Nevertheless, the magnetic parameters were higher for the configuration with the magnetic field oriented in the radial direction of coaxial core-shell structures as compared to the orientation along the nanowire axis, which is in contrast with the behavior previously observed in smaller diameters crystalline ferromagnetic nanotubes. Taking into account that arrays of GaAs nanowires with predominant orientation either perpendicular or parallel to the substrate surface can be produced by a simple anodization procedure, depending on the crystallographic orientation of the GaAs substrate, one can suggest that the obtained results may enlarge opportunities for exploration of magnetic properties of coaxial core-shell structures and widen the area of their applications.

Acknowledgements. This research was funded by National Agency for Research and Development of Moldova under the Grants #20.80009.5007.20 and #20.80009.5007.02, and by European Commission

under the H2020 grant #810652 'NanoMedTwin'. E.V.M. acknowledges support from the Alexander von Humboldt Foundation. V.M. acknowledges support from the German Academic Exchange Service for DAAD scholarship at IFW Dresden (Germany). The authors acknowledge Sabine Neitsch for help with measurements.

REFERENCES

1. H. Mohammed, J. A. Moreno, J. Kosel, Advanced Fabrication and Characterization of Magnetic Nanowires. In *Magnetism and Magnetic Materials*, N. Panwar, ed., IntechOpen, London, 2018; Chapter 2. pp. 7–35.
2. L. Piraux, Appl. Sci. **10**, 1832 (2020).
3. J. García, A. M. Manterola, M. Méndez, J. A. Fernández-Roldán, V. Vega, S. González, V. M. Prida, Nanomaterials **11**, 2282 (2021).
4. M. P. Proenca, C. T. Sousa, J. Ventura, J. P. Araujo, Cylindrical magnetic nanotubes: Synthesis, magnetism and applications. In *Magnetic Nano- and Microwires: Design, Synthesis, Properties and Applications*. 2nd ed., M. Vázquez, ed., Publisher: Elsevier Ltd. 2020, Chapter 6, pp. 135–184.
5. Y. T. Chong, D. Gorlitz, S. Martens, M. Y. E. Yau, S. Allende, J. Bachmann, K. Nielsch, Adv. Mater. **22**, 2435–2439 (2010).
6. M. Stano, O. Fruchart, Magnetic nanowires and nanotubes. In *Handbook of magnetic materials*, Publisher: Elsevier B.V. North Holland, 2018, 27, Chapter 3. pp. 155–267.
7. S. Y. Chou, P. R. Krauss, L. Kong, J. Appl. Phys. **79**, 6101–6106 (1996).
8. S. Choudhury, S. Mondal, D. Anulekha, A. Barman, Tunable picosecond magnetization dynamics in ferromagnetic nanostructures. In *21st Century Nanoscience – A Handbook*, Sattler, K.D. ed.; Publisher: CRC Press, 2020. Chapter 21.
9. E. Monaico, I. Tiginyanu, V. Ursaki, Semicond. Sci. Technol. **35**, 103001 (2020).
10. I. M. Tiginyanu, V. V. Ursaki, E. Monaico, M. Enachi, V. V. Sergentu, G. Colibaba, D. D. Nedeoglo, A. Cojocaru, H. Föll, J. Nanoelectronics and Optoelectronics **6**, 463–472 (2011).
11. E. V. Monaico, E. I. Monaico, V.V. Ursaki, I. M. Tiginyanu, K. Nielsch, Surf. Eng. Appl. Electrochem. **55**, 367–72 (2019).
12. I. Tiginyanu, E. Monaico, E. Monaico, Electrochem. Commun. **10**, 731–734 (2008).
13. E. I. Monaico, E. V. Monaico, V. V. Ursaki, S. Honnali, V. Postolache, K. Leistner, K. Nielsch, I. M. Tiginyanu, Beilstein J. Nanotechnol. **11**, 966–975 (2020).
14. E. V. Monaico, V. Morari, V. V. Ursaki, K. Nielsch. I. M. Tiginyanu, Nanomaterials **12**, 1506 (2022).
15. K. Leistner, K. Duschek, J. Zehner, M. Yang, A. Petr, K. Nielsch, K.L. Kavanagh, Role of Hydrogen Evolution during Epitaxial Electrodeposition of Fe on GaAs. J. Electrochem. Soc., 165, H3076–H3079 (2018).
16. A. L. Kozlovskiy, I. V. Korolkov, M. A. Ibragimova, M. V. Zdorovets, M. D. Kutuzau, L. N. Nikolaevich, E. Y. Kaniukov, Nanotechnologies in Russia **13**, 331–336 (2018).
17. I. Minguez-Bacho, S. Rodriguez-López, M. Vázquez, M. Hernández-Vélez, K. Nielsch, Nanotechnology **25**, 145301 (2014).
18. M. Daub, J. Bachmann, J. Jing, M. Knez, U. Gösele, S. Barth, S. Mathur, J. Escrig, D. Altbir, K. Nielsch, ECS Trans. **11**, 139–148 (2007).
19. M. Daub, M. Knez, U. Goesele, K. Nielsch, J. Appl. Phys. **101**, 09J111 (2007).
20. R. Zierolda, K. Nielsch, ECS Trans. **41**, 111–121 (2011).
21. O. Albrecht, R. Zierold, S. Allende, J. Escrig, C. Patzig, B. Rauschenbach, K. Nielsch, D. Gorlitz, J. Appl. Phys. **109**, 093910 (2011).